A Decline in Marine Biodiversity Caused by Pollution May Be a Primary Driver of Climate Disruption

GOES Foundation multi-vessel image survey of the North Atlantic, 2021–2023

Dr. Howard Dryden and Diane Duncan, with the GOES Foundation community-science consortium and participating vessel crews

Seahorse Point Nature laboratory
Bastimentos
Bocas del Toro
Panama
www.seahorsepoint.org

Abstract

Climate policy treats carbon dioxide as the single lever on the climate. We suggest a second one has been overlooked: the marine biodiversity that builds and maintains the ocean surface microlayer (SML), and that pollution is now degrading[1]. Water vapour, not CO_2, is the largest single contributor to the natural greenhouse effect and the strongest feedback on warming[2]. The ocean supplies most of that vapour across the 71% of the planet it covers, and the thin lipid-and-surfactant film phytoplankton spread over the sea surface helps govern how readily it evaporates and forms aerosol[1,3]. That same film gathers lipophilic ‘forever’ chemicals, together with the microplastic and black-carbon soot they cling to, to levels far above the water beneath, where they turn toxic to the plankton that hold the ecosystem together[4,5,6].

An automated image pipeline sized and classified 51,547 particles larger than 20 µm in 352 georeferenced surface samples from eight sailing vessels. Zooplankton were absent from 93.8% of stations. Black carbon appeared at 89.8%, microplastic particles at 69.9%, microfibres at 22.4% and phytoplankton at 81.8%; 99.2% of everything counted measured below 200 µm. The crews’ own counts and a separate set of GPS-tagged images told the same story, and a plankton net towed by day and by night confirmed it directly, returning roughly 0.2 to 0.5 animals per cubic metre — far below any productive ocean. In short, this surface layer is stripped of animal plankton and steeped in combustion and plastic residue. We trace what that may mean for the microlayer, for water-vapour feedback and cloud formation, and for ocean pH, and argue that cutting pollution has to sit beside cutting carbon.

Keywords: climate; plankton; marine biodiversity; pollution; black carbon; microplastic; surface microlayer.

Highlights

The report details the very first survey, to our knowledge, to measure plankton and microplastics together along a zonal (east–west) Atlantic transect parallel to the equator from North Africa to the Caribbean; open-ocean plankton surveys for this region are otherwise rare and run north–south.

A citizen-science survey now resolves 51,547 surface particles at 352 georeferenced North Atlantic stations.

Zooplankton were absent from 93.8% of stations; the surface ocean along the trade-wind crossing is effectively devoid of animal plankton larger than 20 µm.

Black carbon (89.8% of stations) and microplastic (69.9%) are near-ubiquitous and dominate a particle field in which 99.2% of objects are below 200 µm[7,8,9,10,11,12].

Pollutant load rises sharply toward South America, consistent with terrestrial and riverine input[13].

The SML regulates water-vapour pressure, cloud formation and precipitation; its loss, driven by plankton decline, points to climate disruption that carbon mitigation alone cannot prevent[1,2,14].

Eliminating black carbon, lipophilic toxic chemicals and plastic is therefore a climate measure, not only a pollution measure[7,15].

1. Introduction

Every ocean wears a surface microlayer: a distinct skin, somewhere between 1 and 1000 µm thick[16], made of proteins, carbohydrates and lipids from marine plankton and laced with particulate matter, sub-micron and microplastic, black-carbon soot and chelated metals[1,3,17]. It is not inert. The SML is a living biofilm — bacteria and nanoplankton suspended in a mucopolysaccharide gel with the lipids and surfactants — and it damps turbulence, throttles gas exchange, seeds aerosols and clouds, and slows the escape of water from the sea surface[1,14].

Water vapour is the largest single contributor to the natural greenhouse effect and the strongest feedback on CO_2-driven warming. Its abundance climbs with temperature, through the Clausius–Clapeyron relation, but what happens at the air–sea boundary matters too[2]. Our proposition is simple: the SML is a second, biologically maintained control on that boundary, plankton keep it in repair, and pollution is wearing it away. What follows sets out the survey evidence for the loss of plankton and the build-up of pollutants, then follows the possible consequences through the microlayer to moisture exchange, clouds, ocean pH and biodiversity.

2. The GOES North Atlantic survey: image analysis

Surface water is the layer that holds most particles and toxic chemicals, yet conventional oceanography samples mainly from 5–200 m depth and rarely resolves the 20 µm fraction in mid-ocean. The GOES citizen-science project was designed to fill that gap. Crews on ocean-going yachts drew surface samples on a fixed schedule (12:00 hrs and 24:00 hrs), filtered them to ~20 µm, and photographed the filter under a microscope whose maximum magnification places a single 5 mm aperture (5000 µm) across the field of view, giving an imaging resolution of about 20 µm. Systematic plankton surveys of the open equatorial Atlantic are sparse: the principal effort, the Atlantic Meridional Transect, runs meridionally, north to south[18,19], and quantitative zooplankton surveys have been

described as effectively absent in the equatorial and South Atlantic[20]. To our knowledge, no previous survey has measured plankton and microplastics together along a zonal transect, parallel to the equator, from North Africa to the Caribbean — the gap this survey was designed to fill.

We assembled the recoverable photographic archive from 8 vessels sampling between 2021 and 2023 along the trade-wind route from the Canary Islands and Cape Verde to the Caribbean and Suriname, with higher-latitude return legs. An automated pipeline (OpenCV) locates the filter aperture, detects every particle larger than 20 µm, measures it against the known 5 mm field width, and classifies it as zooplankton, phytoplankton, plastic particle, plastic fibre or black (combustion) carbon. Each image was tied to a position from its GPS tag or its field-log row. In total the pipeline sized and classified 51,547 particles at 352 georeferenced stations.

2.1 Near-absence of zooplankton

The dominant result is an absence. Zooplankton were not detected at 93.8% of stations, and the entire archive yielded only 44 animal-class objects — the largest things measured (median 328 µm). The absence was not confined to any vessel or region (Fig. 1), and an independent set of 110 GPS-tagged images from a single crossing returned no zooplankton at any point on the track (Fig. 2). Microplastic ingestion and pollutant toxicity can suppress copepods and other grazing zooplankton[9,21,22,23,24,25]; a long-term decline in phytoplankton has also been reported, although its magnitude remains debated[26]. An independent net-tow survey, by day and by night, confirmed this scarcity directly (§2.6).

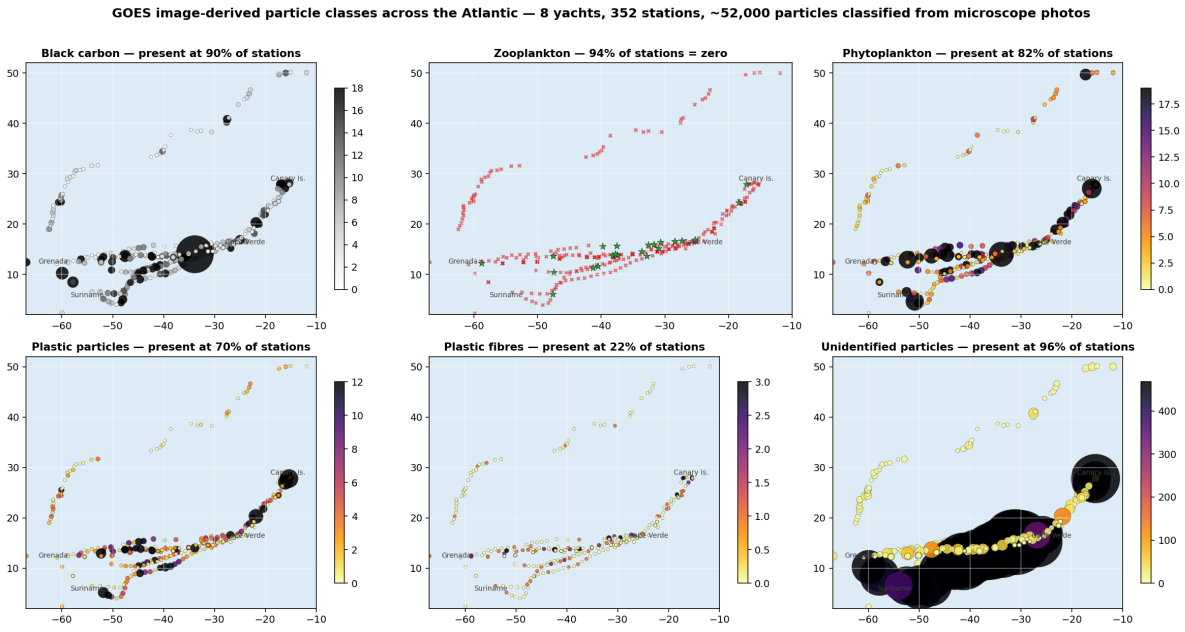

Fig. 1. Image-derived particle classes across the North Atlantic (8 vessels, 352 stations). Zooplankton (top-left) are absent at most stations; black carbon, phytoplankton and plastic recur throughout.

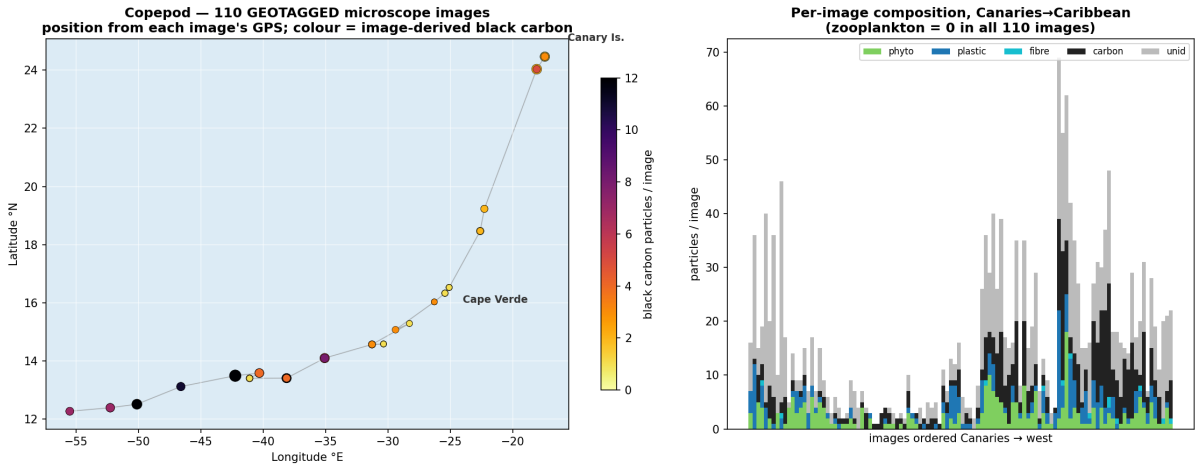

Fig. 2. Geotagged single-vessel sub-survey (110 images, GPS per image). Left: track coloured by image-derived black carbon. Right: per-image composition; zooplankton absent from all 110 images.

2.2 Ubiquitous black carbon and microplastic

Against that empty animal background, anthropogenic particles were near-universal. Black carbon was present at 89.8% of stations (3,559 particles; median 31 µm), microplastic particles at 69.9% and microfibres at 22.4% (median fibre length 204 µm). Phytoplankton-class objects were present at 81.8% of stations. Plastic and black carbon are now documented throughout the open ocean, including the Atlantic water column, the remote marine atmosphere and polar snow[7,8,9,10,11,12,27], so the pervasiveness seen here is expected. Expressed as concentrations (Table 1; each 5 mm field passes ~100 mL, so per-litre = particles per field × 10), black carbon spanned about 0–52 /L (median 12, maximum ~1,304), phytoplankton 0–50 /L and microplastic particles 0–40 /L, while zooplankton stayed at or near zero. Load increased markedly toward the western basin and the South American shelf, the direction of greatest river and terrestrial input[13] (Fig. 3).

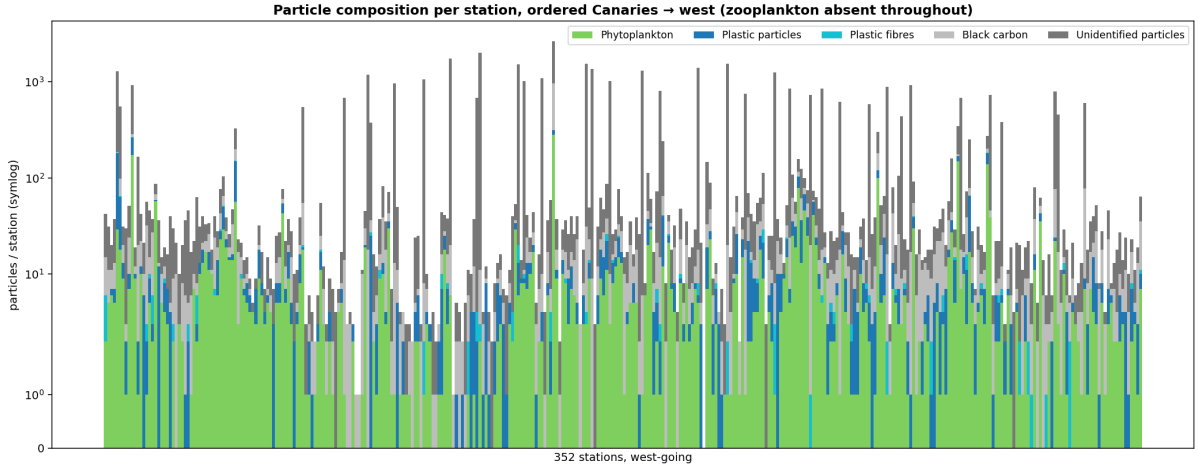

Fig. 3. Per-station particle composition ordered west from the Canary Islands. Zooplankton are flat at zero; carbon, plastic and unidentified material dominate and rise toward South America.

2.3 The surface field is overwhelmingly sub-200 µm

The particle field was very small: 99.2% of all classified particles measured below 200 µm, bunched against the 20 µm filtration and imaging limit (Fig. 4). Plastic fibres formed a distinct larger mode (median 204 µm) and the rare zooplankton occupied the >200 µm range. Because abundance is concentrated at the smallest resolvable size, the true particle burden — including the submicron fraction that the SML preferentially binds — is certainly higher than these counts, which should be read as a floor.

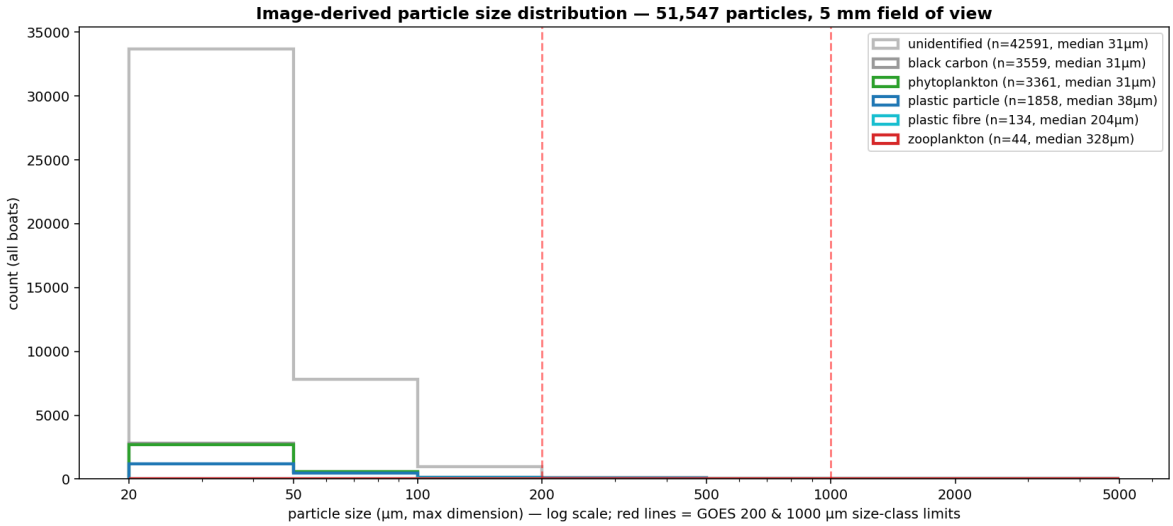

Fig. 4. Image-derived particle size distribution by class (log axis; dashed lines mark the 200 and 1000 µm boundaries).

2.4 Validation and limitations of the classification

We validated the pipeline against one vessel leg counted by hand. The two agreed on the points that carry this paper: zero zooplankton at every station, and a load dominated by carbon and fine unresolved material (Fig. 5). They diverged on the split between plastic and phytoplankton, where the algorithm leaned toward plastic and the human toward phytoplankton. We therefore treat the zooplankton-absence and total-load signals as firm and the plastic-versus-algae partition as provisional. ‘Black carbon’ here is an optical description — dark, colourless particles — and could include sediment, shadow or dark plastic; confirming its composition requires spectroscopy. These are microscope images from an opportunistic citizen-science programme without blank controls or standardised optics, so fibre counts in particular may include airborne contamination, and only the 20 µm–5 mm window was imaged. The filter tube was covered by a cap; only when the filter paper was removed from the assembly would there be a risk of contamination. It is, therefore, considered to be minor.

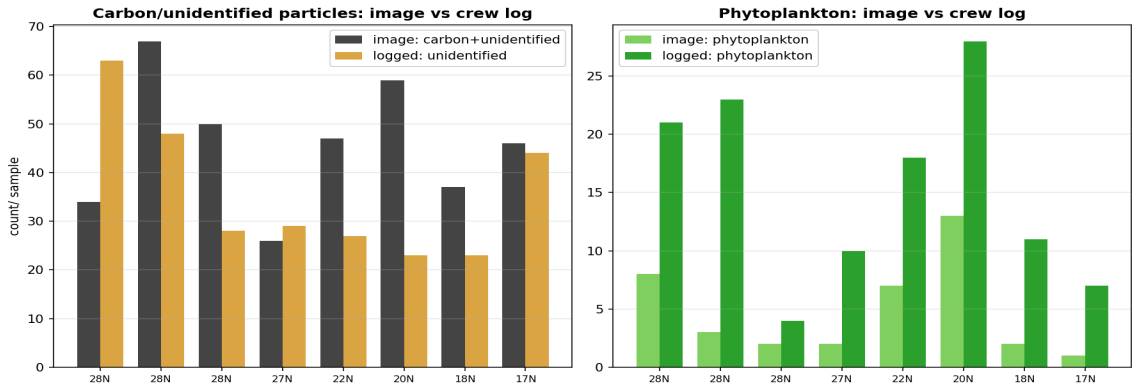

Fig. 5. Automated versus hand counts for one leg. Carbon and total load track the human counter closely; the plastic-versus-phytoplankton split is the main disagreement.

2.5 Survey at a glance

Metric / class	This revision — stations	This revision — particles per litre
Vessels	8 (2021–2023)	—
Images / particles	51,547 classified	—
Georeferenced stations	352	—
Zooplankton (>20 µm)	absent at 93.8%	≈0 /L typical (max 22)
Zooplankton (net tow, day)	present in all 10 tows	≈0.22 /m³ ≈ 1 per 4,500 L
Zooplankton (net tow, night)	present in all 4 tows	≈0.46 /m³ ≈ 1 per 2,180 L
Phytoplankton (>20 µm)	present at 81.8%	0–50 /L (median 10, max 562)
Black carbon	present at 89.8%	0–52 /L (median 12, max 1304)
Plastic particles	present at 69.9%	0–40 /L (median 5, max 378)
Plastic fibres	present at 22.4%	0–2 /L (median 0, max 20)
All particles	—	0–130 /L (median 35)
Size structure	99.2% of particles < 200 µm	—

Table 1. Survey at a glance. Per-litre concentrations are derived from the image counts on the basis that each 5 mm filter field passes ~100 mL of seawater (per-litre = particles per field × 10); ranges span the 10th–90th percentile across stations, with median and maximum in parentheses. These counts include only particles ≥20 µm resolved in the imaged field and are therefore conservative; the lower black-carbon figures relative to the 2022 estimate (100–1000 /L) reflect this resolution limit and the exclusion of the sub-20 µm fraction the SML preferentially binds.

2.6 Independent confirmation by net tow, day and night

To test whether the near-absence of zooplankton in the surface grab samples was an artefact of the small sampled volume, a concentrating plankton net was towed in the mid-Atlantic. A 120 µm mesh net of 0.30 m mouth diameter was towed at 1 to 2 knots for 10 minutes per haul; each haul therefore strained roughly 43,600 litres (mouth area 0.071 m² × ~617 m towed). Because many zooplankton migrate downward by day and rise toward the surface at night, the net was towed in two sets: ten hauls in daylight (12:00–15:00) and four after dark.

Zooplankton were recovered in every haul. The ten daytime hauls returned 5, 10, 2, 13, 4, 7, 27, 6, 9 and 14 individuals (97 in ~436,000 litres), a concentration of about 0.22 per cubic metre, or one animal per 4,500 litres. The four night hauls returned 25, 15, 32 and 8 (80 in ~175,000 litres), about 0.46 per cubic metre, or one per 2,180 litres (Table 2). The night surface density is roughly twice the daytime value, exactly the pattern expected from diel vertical migration — but the decisive point is that even at night, when surface-living and migrating zooplankton are both present, the standing stock is only about half an individual per cubic metre.

This removes the main alternative explanation for the image survey: the surface scarcity is not simply an effect of small sample volume. Two methodological caveats remain — the 120 µm mesh retains larger taxa while passing the smallest copepods and nauplii, and filtered volume is computed from tow geometry rather than a flow-meter — so the standardised, replicated net sampling recommended below would refine the absolute figures. A surface zooplankton stock of 0.2–0.5 per cubic metre, day and night, nonetheless sits far below densities typical of productive open ocean.

Net tow (120 µm, 0.30 m, ~2 kn × 10	Daytime (12:00–15:00)	Night
Number of hauls	10	4
Zooplankton per haul	5, 10, 2, 13, 4, 7, 27, 6, 9, 14	25, 15, 32, 8
Mean per haul	9.7	20.0
Total caught / volume filtered	97 in ≈436,000 L	80 in ≈175,000 L
Concentration	≈0.22 m^{-3}	≈0.46 m^{-3}
Equivalent	≈1 per 4,500 L	≈1 per 2,180 L

Table 2. Net-tow confirmation of zooplankton scarcity by day and night (mid-Atlantic). Filtered volume is the swept volume of the net mouth (area × tow distance); concentrations assume complete filtration and are therefore upper-bound counts per unit volume. Night density is ~2× daytime, consistent with diel vertical migration, yet remains below 0.5 m^{-3}.

2.7 Lessons and protocol refinements

The constraints noted above reflect the realities of sampling from small sailing vessels, and each has already translated into a specific improvement for the next campaign rather than a gap in the present one. Retaining and preserving the filter papers for later laboratory analysis was not practical in the limited, often damp storage aboard the yachts; filter retention and preservation, followed by FTIR/Raman confirmation of the plastic and carbon particles, has therefore been written into the sampling protocol for future crossings. The net tows were likewise an opportunistic addition to the imaging survey: towing a plankton net safely from a small yacht is not routine, and holding a steady tow speed under sail is difficult, so the tow figures are reported here as preliminary. Future work will use a flow-metered net at a controlled speed (motor-assisted where possible), with replicate day and night hauls at each station. These refinements are the natural product of a first-generation, proof-of-concept design: the citizen-science method is deliberately low-cost and scalable, and the survey reported here establishes both the signal and the practical method that a standardised programme can now build upon.

3. Sources of marine pollution and their implications

The SML attracts lipophilic ‘forever’ chemicals, microplastics and hydrophobic black-carbon soot from the incomplete combustion of fossil fuels and biomass. Measured concentrations of toxic chemicals in the SML can be many times higher than in the water below[4], so the layer acts as an accumulator at the precise interface where plankton live. Hydrophobic black carbon and plastic particles preferentially adsorb these lipophilic chemicals and can carry them into the base of the food web[6,7];

partially combusted carbon behaves much like plastic in this respect, a point that has been largely overlooked. Both classes are present across the open Atlantic far from land[8,9], so this is an open-ocean phenomenon, not only a coastal one.

4. The surface microlayer, aerosols, clouds and evaporation

The SML is built from phytoplankton lipids and surfactants[3,28]. It feeds the marine aerosols that clouds condense upon[14], and at the same time it slows evaporation and the loss of heat to the air[2]. A healthy film, then, cools the surface, encourages cloud and rain, and keeps humidity in check. Strip it away and evaporation and water vapour can rise while cloud cover falls. Since the ocean supplies almost all of that atmospheric moisture, the physical and biological condition of the sea surface is a climate variable in its own right, and one that carbon-only models leave out.

5. Ecosystem regime shift and ocean acidification

Toxic loading affects grazing zooplankton[21,22]; the survey's near-total absence of animals is consistent with heavy grazer loss, after which phytoplankton may bloom and sink un-grazed. Separately, large parts of the open ocean are high-nutrient, low-chlorophyll (HNLC): there, macronutrients remain abundant but phytoplankton growth is limited chiefly by iron, so productivity stays low despite available nutrients[29]. As primary production changes, less carbon may be fixed at the surface and dissolved CO_2 rises; microplastic loading may itself further weaken the biological carbon pump[30].

The coccolithophores and diatoms that build the SML are also among the plankton least able to tolerate falling pH[31,32]; lose them and the film thins further, tightening a loop between acidification, plankton loss and evaporation. On present trends, surface pH could fall below about 7.95 within a few decades[31]. Acidification is a serious and, in places, underrated consequence of rising CO_2. Whether these strands could tighten into a basin- or ocean-scale regime shift, and how quickly, is genuinely uncertain, and the present data do not settle it. The direction of travel, though, is reason enough for concern about ocean productivity and the wider Earth system.

Sargassum

There should be in the region of 1 to 2 million tonnes of Sargassum crossing the equatorial Atlantic from Africa to the Caribbean. However, due to eutrophication from the Amazon, Gambia and Congo rivers, together with nutrient-rich run-off, the biomass of the Great Atlantic Sargassum Belt is now of the order of tens of millions of tonnes[33,34]. Yacht Copepod and other yachts in the project were frequently caught in giant mats of this pelagic macrophyte. The Sargassum competes with phytoplankton for phosphate and other nutrients[34]. As phosphate concentrations fall to low levels, Sargassum increasingly takes up arsenate in place of phosphate, so that by the time it reaches the Caribbean the tissue is heavily loaded with arsenic[35]. While water analysis was not conducted, it can be inferred that phosphate concentrations along the belt are extremely low, with consequent effects on the growth of phytoplankton and the zooplankton that depend upon them.

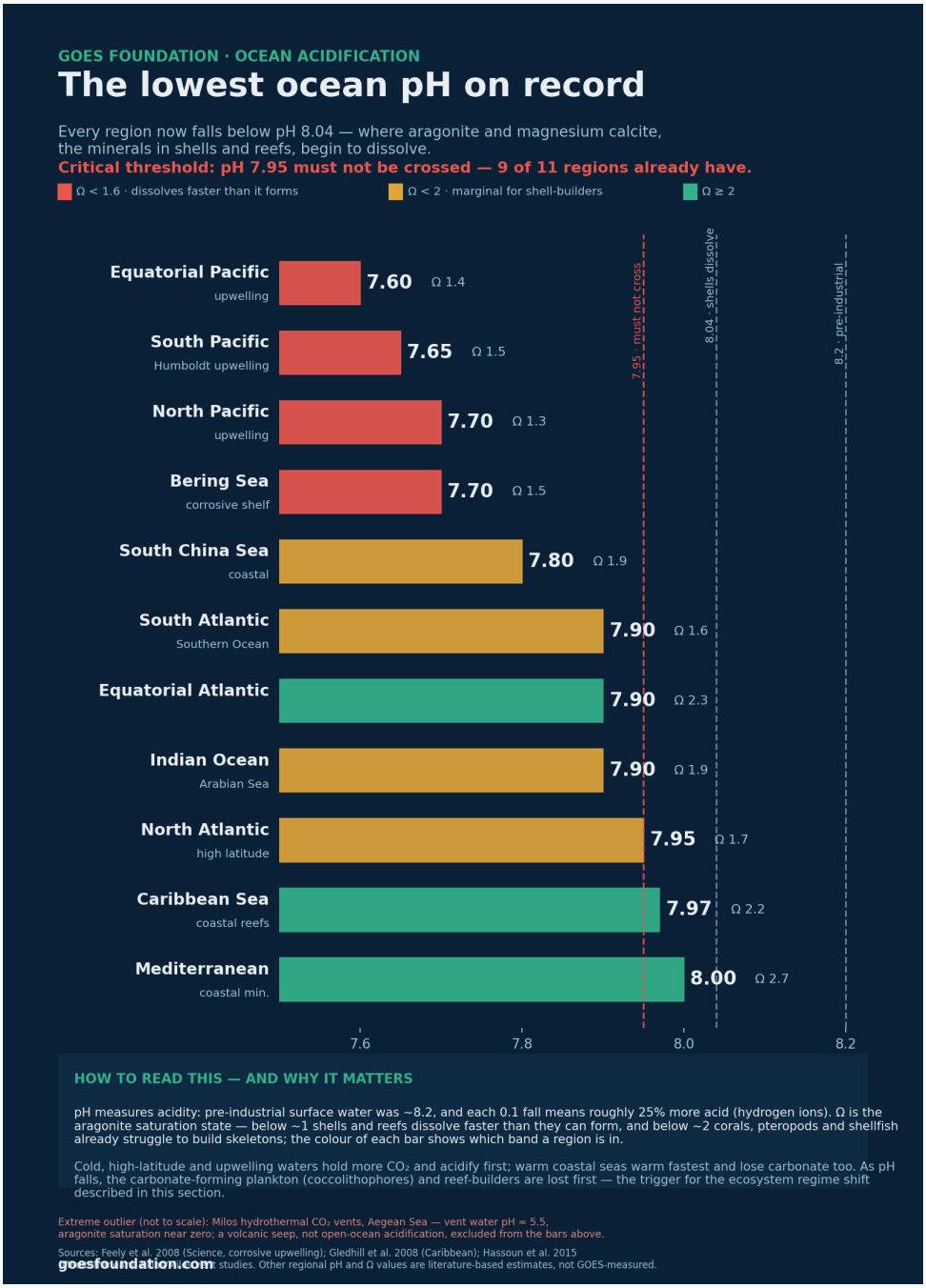

Figure 6. Regional surface / upwelled seawater pH with aragonite saturation state (Ω). Carbonate (aragonite / high-Mg calcite) dissolution is governed by the saturation state Ω — dissolution where Ω < 1 — which depends on pH together with temperature, dissolved inorganic carbon and alkalinity; the pH values shown are indicative regional levels, not fixed dissolution thresholds. Named sources: corrosive upwelling shelves (Equatorial/North/South Pacific, Bering)[36]; Greater Caribbean[37]; Mediterranean[38]; Milos CO_2-vent outlier[39]. Remaining regional pH and Ω values are literature-based estimates, not measured at GOES stations.

Duration of exposure, multiple stressors and the risk of a regime shift

The pH values shown in Figure 6 are the lowest, transient minima recorded, not long-term averages. Their biological significance depends on how long these low-pH events persist: brief excursions may be tolerated, but sustained exposure reduces the fecundity and survival of plankton and other calcifying organisms, and the effect is amplified where acidification coincides with warming[40]. Even where organisms survive, they are physiologically stressed, and this stress acts together with the toxic-chemical and particulate load documented earlier in this report; such multiple stressors interact and can compound one another[5,40], and stressed plankton are expected to become more susceptible to infection and disease.

Sustained acidification and warming also restructure the plankton community, reducing the proportion of diatoms and favouring dinoflagellates[41]. Consistent with large-scale change, more than half of the global ocean — approximately 56% — has become measurably greener over the past two decades, a climate-change signal in ocean colour that reflects shifting phytoplankton ecosystems[42]. GOES interprets these converging trends as an early warning of a possible large-scale regime shift, away from the diatoms and calcifying plankton that anchor the marine food web and help maintain the surface microlayer. Whether such a shift could unfold within a decade is uncertain and is not established by the present evidence; but its direction — toward a less productive, dinoflagellate-dominated surface ocean — represents a serious risk to ocean productivity and, through it, to the wider Earth system[43].

6. Carbon dioxide and marine biodiversity

Carbon dioxide still matters. Even at net zero, the CO_2 already in the air would keep acidifying the ocean, and that is chemistry this survey cannot undo[31,44]. The case here is additive, not dismissive: cutting carbon is necessary, but on its own it is not enough. Leave in place the pollution harming surface plankton, and the SML may keep degrading. Enhanced weathering — spreading finely ground silicate minerals such as olivine on farmland to draw down CO_2 and raise ocean alkalinity, with iron and silica that might in principle favour diatoms — has been proposed, but its scale (1 to 10 billion tonnes), cost (approx $40/tonne) and ecological side-effects remain highly uncertain, and we raise it only as something to be evaluated, not as a solution in hand.

7. Conclusion

Across 352 stations and 51,547 classified particles, the trade-wind Atlantic surface held almost no animal plankton above 20 µm, a great deal of combustion and plastic residue, and a particle field dominated by its smallest sizes. Not every step in the SML hypothesis is settled. But a surface ocean this empty of plankton and this laden with anthropogenic particles is a stressed system, and stressed systems of this kind are the ones that tip[43,45].

Emissions must fall, and urgently. But carbon mitigation alone will not halt ocean acidification or rebuild the SML. The discharge of black carbon, lipophilic ‘forever’ chemicals and plastic has to fall as well. Pollution already ranks among the largest environmental causes of early human death, and ocean pollution is a recognised hazard to health[15,46]. Plankton, for their part, underpin ocean productivity and rebound quickly once the pressure eases: the majority of marine biomass — roughly 60%

— is smaller than 1000 µm[47], and such small plankton can double within days[48]. On this evidence, restoring marine life belongs alongside decarbonisation, not behind it.

8. Recommendations

Continue and accelerate carbon mitigation, but treat pollution elimination as a parallel climate measure of equal urgency.

Eliminate discharge of lipophilic ‘forever’ chemicals, plastic and black-carbon soot; treat all wastewater; adopt a ‘do no harm’ and try and do some good standard for land and ocean.

Transition from destructive farming and unsustainable fishing toward rewilding and ecosystem regeneration on land and at sea.

Evaluate raising seawater alkalinity — for example through limestone or silicate minerals such as olivine dispersal on land — as a potential means of buffering surface ocean pH, subject to full assessment of its efficacy and ecological side-effects.

Establish standardised, calibrated surface-microlayer monitoring — building on the citizen-science method here but adding laboratory particle confirmation (FTIR/Raman), procedural blanks and replication — to convert these observations into quantitative time series; and evaluate complementary remote sensing, such as synthetic-aperture radar of sea-surface roughness, to map the microlayer and surface pollution at basin scale.

Methods (survey analysis)

Surface samples were collected by participating crews at ~12-hour intervals (12:00hrs and 24:00hrs), filtered to ~20 µm, and photographed on digital microscopes at a 5 mm field of view, with position, date and time logged. Positions were taken from image GPS (read from the HoudahGeo database for the geotagged subset) or from the field spreadsheet via the workbook image anchors; mixed degree/decimal-minute coordinates were converted to decimal degrees, with unmarked longitudes assigned West for the survey region. Images were analysed in OpenCV: Hough-circle aperture detection, then segmentation by combined background-subtraction and saturation thresholds; connected components ≥20 µm (max dimension, scaled by 5 mm / image width) were classified by elongation, saturation, hue and darkness, with unresolved objects left unidentified, and every particle sized. The pipeline was validated against one hand-counted leg. Per-station counts, all particle sizes and the crew logs accompany this paper as a supplementary workbook (GOES_ALL_DATA.xlsx).

Net-tow validation: a 120 µm plankton net (0.30 m mouth) was towed at ~2 knots for 10 min per haul — ten daytime hauls (12:00–15:00) and four night hauls, mid-Atlantic; filtered volume was computed as net mouth area × tow distance and zooplankton in each haul counted and expressed per unit volume.

Data availability

The per-station particle counts, the individual particle-size measurements and the crew field logs that support this study are provided in the supplementary workbook (GOES_ALL_DATA.xlsx) and are available from the corresponding author on reasonable request.

Author contributions

H.D. conceived and led the GOES project, designed the sampling protocol, and led the analysis and writing. D.D. contributed to the study design and to the manuscript. The participating vessel crews collected the field samples and microscope images. All authors reviewed and approved the final manuscript.

Competing interests

The authors are associated with the GOES Foundation, a not-for-profit organisation. They declare no financial competing interests.

AI-assistance statement

The data analysis, figure generation and drafting of this manuscript were carried out with the assistance of a generative-AI system (Anthropic's Claude). The automated image-analysis pipeline, statistical summaries and text were produced with AI support and then reviewed by the authors. All data, interpretations and conclusions are the authors' own; the authors verified the analyses and references and take full responsibility for the content.

References

1. Cunliffe, M. et al. Sea surface microlayers: a unified physicochemical and biological perspective. *Prog. Oceanogr.* **109**, 104–116 (2013).

2. Held, I. M. & Soden, B. J. Water vapor feedback and global warming. *Annu. Rev. Energy Environ.* **25**, 441–475 (2000).

3. Garrett, W. D. The organic chemical composition of the ocean surface. *Deep-Sea Res.* **14**, 221–227 (1967).

4. Wurl, O. & Obbard, J. P. A review of pollutants in the sea-surface microlayer (SML): a unique habitat for marine organisms. *Mar. Pollut. Bull.* **48**, 1016–1030 (2004).

5. Tetu, S. G. et al. Plastic leachates impair growth and oxygen production in Prochlorococcus, the ocean's most abundant photosynthetic bacteria. *Commun. Biol.* **2**, 184 (2019).

6. Ziccardi, L. M., Edgington, A., Hentz, K., Kulacki, K. J. & Kane Driscoll, S. Microplastics as vectors for bioaccumulation of hydrophobic organic chemicals in the marine environment. *Environ. Toxicol. Chem.* **35**, 1667–1676 (2016).

7. Bond, T. C. et al. Bounding the role of black carbon in the climate system. *J. Geophys. Res. Atmos.* **118**, 5380–5552 (2013).

8. Cózar, A. et al. Plastic debris in the open ocean. *Proc. Natl Acad. Sci. USA* **111**, 10239–10244 (2014).

9. Pabortsava, K. & Lampitt, R. S. High concentrations of plastic hidden beneath the surface of the Atlantic Ocean. *Nat. Commun.* **11**, 4073 (2020).

10. Allen, S. et al. Atmospheric transport and deposition of microplastics in a remote mountain catchment. *Nat. Geosci.* **12**, 339–344 (2019).

11. Bergmann, M. et al. White and wonderful? Microplastics prevail in snow from the Alps to the Arctic. *Sci. Adv.* **5**, eaax1157 (2019).

12. Trainic, M. et al. Airborne microplastic particles detected in the remote marine atmosphere. *Commun. Earth Environ.* **1**, 64 (2020).

13. Mai, L. et al. Global riverine plastic outflows. *Environ. Sci. Technol.* **54**, 10049–10056 (2020).

14. O'Dowd, C. D., Smith, M. H., Consterdine, I. E. & Lowe, J. A. Marine aerosol, sea-salt and the marine sulphur cycle. *Atmos. Environ.* **31**, 73–80 (1997).

15. Fuller, R. et al. Pollution and health: a progress update. *Lancet Planet. Health* **6**, e535–e547 (2022).

16. Zhang, Z. et al. Direct determination of thickness of the sea-surface microlayer using a pH microelectrode at original location. *Sci. China Ser. B* **46**, 339–351 (2003).

17. Williams, P. M. et al. Chemical and microbiological studies of sea-surface films in the Southern Gulf of California. *Mar. Chem.* **19**, 17–98 (1986).

18. Aiken, J. et al. The Atlantic Meridional Transect: overview and synthesis of data. *Prog. Oceanogr.* **45**, 257–312 (2000).

19. Woodd-Walker, R. S., Ward, P. & Clarke, A. Large-scale patterns in the diversity and community structure of surface zooplankton across a 20°W meridional transect of the NE Atlantic. *Deep-Sea Res. II* **47**, 2903–2924 (2000).

20. Vereshchaka, A. L. et al. The deep-sea zooplankton of the North, Central, and South Atlantic: biomass, abundance and diversity. *Deep-Sea Res. II* **137**, 89–101 (2017).

21. Desforges, J.-P., Galbraith, M. & Ross, P. S. Ingestion of microplastics by zooplankton in the northeast Pacific Ocean. *Arch. Environ. Contam. Toxicol.* **69**, 320–330 (2015).

22. Ma, H. et al. Microplastics in aquatic environments: toxicity to trigger ecological consequences. *Environ. Pollut.* **261**, 114089 (2020).

23. Cole, M. et al. Microplastic ingestion by zooplankton. *Environ. Sci. Technol.* **47**, 6646–6655 (2013).

24. Botterell, Z. L. R. et al. Bioavailability and effects of microplastics on marine zooplankton: a review. *Environ. Pollut.* **245**, 98–110 (2019).

25. Galloway, T. S., Cole, M. & Lewis, C. Interactions of microplastic debris throughout the marine ecosystem. *Nat. Ecol. Evol.* **1**, 0116 (2017).

26. Boyce, D. G., Lewis, M. R. & Worm, B. Global phytoplankton decline over the past century. *Nature* **466**, 591–596 (2010).

27. Aves, A. R. et al. First evidence of microplastics in Antarctic snow. *Cryosphere* **16**, 2127–2145 (2022).

28. O'Dowd, C. D. et al. Biogenically driven organic contribution to marine aerosol. *Nature* **431**, 676–680 (2004).

29. Tyrrell, T. et al. Effect of seafloor depth on phytoplankton blooms in high-nitrate, low-chlorophyll (HNLC) regions. *J. Geophys. Res. Biogeosci.* **110**, G02007 (2005).

30. Shen, M. et al. Can microplastics pose a threat to ocean carbon sequestration? *Mar. Pollut. Bull.* **150**, 110712 (2020).

31. Hönisch, B. et al. The geological record of ocean acidification. *Science* **335**, 1058–1063 (2012).

32. Riebesell, U. et al. Reduced calcification of marine plankton in response to increased atmospheric CO2. *Nature* **407**, 364–367 (2000).

33. Wang, M. et al. The great Atlantic Sargassum belt. *Science* **365**, 83–87 (2019).

34. Lapointe, B. E. et al. Nutrient content and stoichiometry of pelagic Sargassum reflects increasing nitrogen availability in the Atlantic Basin. *Nat. Commun.* **12**, 3060 (2021).

35. McGillicuddy, D. J. Jr et al. Nutrient and arsenic biogeochemistry of Sargassum in the western Atlantic. *Nat. Commun.* **14**, 6205 (2023).

36. Feely, R. A., Sabine, C. L., Hernández-Ayón, J. M., Ianson, D. & Hales, B. Evidence for upwelling of corrosive 'acidified' water onto the continental shelf. *Science* **320**, 1490–1492 (2008).

37. Gledhill, D. K., Wanninkhof, R., Millero, F. J. & Eakin, C. M. Ocean acidification of the Greater Caribbean Region 1996–2006. *J. Geophys. Res. Oceans* **113**, C10031 (2008).

38. Hassoun, A. E. R. et al. Acidification of the Mediterranean Sea from anthropogenic carbon penetration. *Deep-Sea Res. I* **102**, 1–15 (2015).

39. Dando, P. R. et al. Gas venting rates from submarine hydrothermal areas around the island of Milos, Hellenic Volcanic Arc. *Cont. Shelf Res.* **15**, 913–929 (1995).

40. Kroeker, K. J. et al. Impacts of ocean acidification on marine organisms: quantifying sensitivities and interaction with warming. *Glob. Change Biol.* **19**, 1884–1896 (2013).

41. Dutkiewicz, S. et al. Impact of ocean acidification on the structure of future phytoplankton communities. *Nat. Clim. Change* **5**, 1002–1006 (2015).

42. Cael, B. B., Bisson, K., Boss, E., Dutkiewicz, S. & Henson, S. A. Global climate-change trends detected in indicators of ocean ecology. *Nature* **619**, 551–554 (2023).

43. Beaugrand, G. et al. Prediction of unprecedented biological shifts in the global ocean. *Nat. Clim. Change* **9**, 237–243 (2019).

44. Jiang, L.-Q. et al. Surface ocean pH and buffer capacity: past, present and future. *Sci. Rep.* **9**, 18624 (2019).

45. IPBES. Global Assessment Report on Biodiversity and Ecosystem Services (IPBES Secretariat, 2019).

46. Landrigan, P. J. et al. Human health and ocean pollution. *Ann. Glob. Health* **86**, 151 (2020).

47. Bar-On, Y. M., Phillips, R. & Milo, R. The biomass distribution on Earth. *Proc. Natl Acad. Sci. USA* **115**, 6506–6511 (2018).

48. Laws, E. A. Evaluation of in situ phytoplankton growth rates: a synthesis of data from varied approaches. *Annu. Rev. Mar. Sci.* **5**, 247–268 (2013).